DALTON
FULL PAPER

Structural and photophysical behaviour of lanthanide complexes with a tetraazacyclododecane featuring carbamoyl pendant arms †

Gaël Zucchi,[a] Rosario Scopelliti,[a] Pierre-André Pittet,[a] Jean-Claude G. Bünzli *[a] and Robin D. Rogers[b]

[a] *Institute of Inorganic and Analytical Chemistry, University of Lausanne, CH-1015 Lausanne, Switzerland. E-mail: Jean-claude.Bunzli@icma.unil.ch*
[b] *Department of Chemistry, The University of Alabama, Tuscaloosa, Alabama, 35487-0336, USA*

Received 3rd December 1998, Accepted 21st January 1999

The crystal and molecular structure of 1,4,7,10-tetrakis(*N*-benzylcarbamoylmethyl)-1,4,7,10-tetraazacyclododecane, L^1, revealed an S_2-symmetric molecule. One pair of pendant arms is involved in intramolecular hydrogen bonding while the other interacts with two other ligand molecules through strong intermolecular hydrogen bonds. In solution, the ligand adopts a similar geometrical arrangement at low temperature but complexes with Eu^{III} and Lu^{III} display an averaged C_4-symmetry on the NMR timescale. One isomer only was detected, as reported for similar complexes, and the arrangement around Eu^{III} and Lu^{III} appears to be rigid while it is more fluxional around La^{III}. Rotation of the benzyl group around the amide function was observed for Eu^{III} and a dynamic NMR study in the range 253–333 K yielded $\Delta H^{\ddagger} = 43.0 \pm 0.1$ kJ mol^{-1}, $\Delta S^{\ddagger} = -49.3 \pm 0.4$ J K^{-1} mol^{-1} and $k^{298} = 47.7 \pm 1.1$ s^{-1}. In the solid state, anhydrous eight-co-ordinate complexes were isolated and high resolution luminescence spectroscopy of Eu^{III} in the europium and Eu-doped compounds of La, Gd and Lu confirmed a site symmetry close to C_4 along the lanthanide-series. Energy transfer from the L^1 $^3\pi\pi^*$ state to the Tb($^5D_4$) excited state is sizable leading to an absolute quantum yield of 6.4% in MeCN, while the Eu^{III} luminescence is only poorly sensitized, possibly because of photoinduced electron transfer processes. The Tb($^5D_4$) and Eu($^5D_0$) lifetimes for both solid state samples and solutions in MeCN are consistent with no water molecule in the inner co-ordination sphere but addition of water results in the ninth co-ordination site being bound to H_2O: number of bound waters, $q = 0.96$ (Eu) and 0.71 (Tb) in MeCN + 2 M H_2O and 1.19 (Eu) and 1.30 (Tb) in water. The relaxivity r_1 of the gadolinium(III) complex is pH dependent and varies between 4.08 (pH 0.8), 1.88 (6.7) and 6.14 (11.1) mM^{-1} s^{-1}.

Introduction

Lanthanide macrocyclic edifices with ligands derived from cyclen (1,4,7,10-tetraazacyclododecane) are being intensively studied in view of their potential applications in biomedical research. These complexes are thermodynamically stable and kinetically inert to the release of lanthanide(III) ions in water. Some of them are used as contrast agents in magnetic resonance imaging (MRI),[1,2] as diagnostic and therapeutic radiopharmaceuticals,[3] as catalysts for the hydrolysis of phosphate diester bonds,[4] or as responsive luminescent lanthanide(III) chelates for the analysis of bioactive ions and molecules.[5,6] Furthermore, the paramagnetism of the lanthanide(III) ions, particularly Eu^{III}, can be taken advantage of to determine the solution structure of their complexes by analysing the lanthanide induced shifts in the NMR spectra.[7]

In addition, complexes of Eu^{III} and Tb^{III} often display useful luminescent properties since the metal ions have easily recognizable narrow emission spectra and long excited state lifetimes, in the millisecond range, provided that the metal ion is efficiently protected from non-radiative deactivation processes.[8] In view of the effectiveness of cyclen derivatives with carbamoyl pendant arms to complex lanthanide ions and to display sizable luminescence,[9] we have launched a research programme with the aim of detecting whether ligands for potential contrast agents could simultaneously yield edifices for the luminescent labelling of biomolecules. Since lanthanide(III) ions have extremely weak molar absorption coefficients, we have chosen a ligand with phenyl moieties to provide chromophoric groups favouring light harvesting and energy transfer onto the metal ion. Ligand L^1 [1,4,7,10-tetrakis(*N*-benzylcarbamoylmethyl)-1,4,7,10-tetraazacyclododecane] features eight co-ordinating donor atoms, satisfying the large co-ordination number requirement of lanthanide(III) ions, while leaving an extra position free for water co-ordination and exchange, a mandatory condition for contrast agents. We expect that the lanthanide ions will be tightly encapsulated between the macrocyclic ring and the pendant arms, as was recently shown for [Eu(L^2)][trif]$_3$ {L^2 is 1,4,7,10-tetrakis[*N*-(1-phenylethyl)-carbamoylmethyl]-1,4,7,10-tetraazacyclododecane, trif = O_3SCF_3}.[10] In this paper we present a solid state and solution study of ligand L^1 and its complexes with Ln(trif)$_3$ (Ln = La, Nd, Eu, Gd or Tb) with particular reference to structural and photophysical properties.

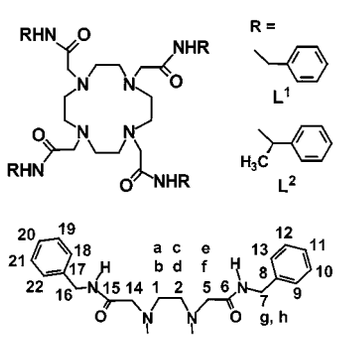

† *Supplementary data available*: least-squares planes, relaxation times, NMR and electronic spectra. For direct electronic access see http://www.rsc.org/suppdata/dt/1999/931/, otherwise available from BLDSC (No. SUP 57491, 12 pp.) or the RSC Library. See Instructions for Authors, 1999, Issue 1 (http://www.rsc.org/dalton).

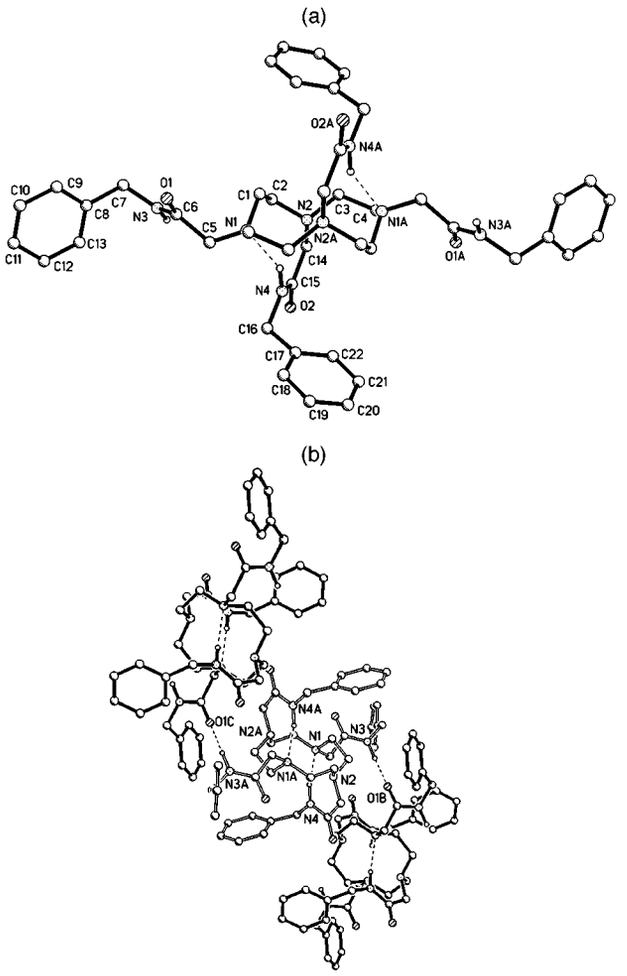

Fig. 1 Molecular structure of L^1 showing the atom-numbering scheme and the intramolecular (a) and interstrand intramolecular (b) hydrogen bonds.

Results and discussion

Solid state and solution structure of L^1

Colourless single crystals of L^1 suitable for X-ray analysis were obtained from acetonitrile. The molecular structure (Fig. 1) is, to the best of our knowledge, the first reported for such a ligand in its free form and confirms the 1,7-*trans* arrangement predicted for similar molecules on the basis of photophysical data.[9b] Selected bond lengths and distances are in Table 1. The molecule lies on a crystallographic inversion centre and displays S_2 symmetry with two sets of equivalent opposite pendant arms. The four-bladed propeller shape of the molecule, with maximum expansion of the pendant arms, results from a network of hydrogen bonds (Table 2) and stacking interactions: (i) one pair of arms are further connected to the 12-membered ring through two intramolecular hydrogen bonds involving the H4 atom of the amide function and N1, N2. The presence of the intramolecular interaction explains why all the atoms belonging to this pair of arms (phenyl ring not included) lie on the same plane: the maximum and minimum deviations from the mean plane are −0.016 (C14) and +0.001 Å (C16) and the interplanar angle with the phenyl ring amounts to 81.3°. (ii) The two other arms are involved in strong intermolecular hydrogen bonding through the H3 atoms of their amide groups and the N3 atoms of two other ligand molecules. The amide functions of these arms are planar, the deviations from the least-squares planes being −0.003 (O1), −0.003 (N3), −0.002 (C5) and 0.008 Å (C6), while the interplanar angle with the least-squares plane of the C8–C13 aromatic ring is 79.8°. (iii) In addition, the C8–C13 aromatic rings face-to-face interact with similar phenyl rings at a C···C stacking distance of about 3.5 Å, while the C17–C22 aromatic rings participate in weaker, edge-to-face interactions with neighbouring chains (closest C···C distance: 4 Å).

Table 1 Selected bond lengths (Å) and angles (°) in L^1

O(1)–C(6)	1.232(4)	O(2)–C(15)	1.237(4)
N(1)–C(5)	1.457(4)	N(1)–C(4)[a]	1.466(4)
N(1)–C(1)	1.473(4)	N(2)–C(14)	1.459(4)
N(2)–C(3)	1.474(4)	N(2)–C(2)	1.480(4)
N(3)–C(6)	1.339(4)	N(3)–C(7)	1.448(4)
N(4)–C(15)	1.344(5)	N(4)–C(16)	1.467(4)
C(1)–C(2)	1.526(5)	C(3)–C(4)	1.522(5)
C(7)–C(8)	1.508(5)	C(5)–C(6)	1.524(5)
C(8)–C(13)	1.395(5)	C(8)–C(9)	1.381(5)
C(10)–C(11)	1.375(5)	C(9)–C(10)	1.385(5)
C(12)–C(13)	1.387(5)	C(11)–C(12)	1.375(5)
C(16)–C(17)	1.496(5)	C(14)–C(15)	1.512(5)
C(17)–C(18)	1.388(5)	C(17)–C(22)	1.382(5)
C(19)–C(20)	1.369(6)	C(18)–C(19)	1.380(5)
C(21)–C(22)	1.389(6)	C(20)–C(21)	1.377(6)
C(5)–N(1)–C(4)[a]	113.5(3)	C(5)–N(1)–C(1)	111.5(3)
C(4)[a]–N(1)–C(1)	114.3(3)	C(14)–N(2)–C(3)	110.8(3)
C(14)–N(2)–C(2)	113.0(3)	C(3)–N(2)–C(2)	111.4(3)
C(6)–N(3)–C(7)	121.4(3)	C(15)–N(4)–C(16)	122.4(3)
N(1)–C(1)–C(2)	111.9(3)	N(2)–C(2)–C(1)	111.1(3)
N(2)–C(3)–C(4)	114.6(3)	N(1)[a]–C(4)–C(3)	112.7(3)
N(1)–C(5)–C(6)	116.7(3)	O(1)–C(6)–N(3)	123.2(3)
O(1)–C(6)–C(5)	121.2(4)	N(3)–C(6)–C(5)	115.6(3)
N(3)–C(7)–C(8)	114.5(3)	N(2)–C(14)–C(15)	115.9(3)
O(2)–C(15)–N(4)	123.7(4)	O(2)–C(15)–C(14)	120.4(4)
N(4)–C(15)–C(14)	115.9(4)	N(4)–C(16)–C(17)	113.5(3)

[a] Symmetry code: $-x+1, -y, -z+1$.

Analysis of the 12-membered ring confirms a double-chair conformation with nitrogen atoms N1, N2 in the upper part while the N atoms generated by the crystallographic inversion centre (N1A, N2A) lie in the lower part (deviations from the mean plane: N1 −0.411, N2 −0.629, C2 +0.023 and C4 +0.025 Å).

At room temperature a solution of L^1 in CD_3OD exhibits ^1H and ^{13}C NMR spectra characteristic of a fluxional species, with respect to arm rotation and ring inversion processes. For instance, the ^{13}C spectrum displays one broad signal for the amide carbon atoms (δ 169.0), four signals for the aromatic carbon atoms (δ 140.3, 130.5, 129.4 and 129.2), one for NCH_2CO (δ 57.3), one broad signal for the ring CH_2 (δ 52.5) and one for CH_2Ph (δ 45.2), pointing to a time-averaged C_4 symmetry. Upon cooling, however, most of the signals become narrow and several split. At 212 K the ^{13}C spectrum is consistent with a diagonal symmetry. More specifically, two sharp signals are observed for the amide carbon atoms, eight for the aromatic carbon atoms, two for each of the methylenic NCH_2CO and CH_2Ph groups, while one broad signal only is observed at δ 52.9 for the ring methylene carbon atoms (Fig. 2). This points to a solution structure close to the one observed in the solid state as far as the pendant arms are concerned, while the ring inversion process is still fast on the NMR timescale at this temperature.

Solution structure of the $[Ln(L^1)][trif]_3$ complexes

Ligand L^1 reacts with lanthanide triflates to yield 1:1 complexes the formulation of which, after drying under vacuum at 333 K, is consistent with anhydrous $[Ln(L^1)][trif]_3$. We note that C_4-symmetric monohydrated complexes of Eu and Dy with L^2 have been evidenced by X-ray crystallography.[10] Complexation is evidenced in the vibrational spectra which show a red shift of the ν(C=O) mode. The presence of a single ν(C=O) stretching band ascertains that the ions are bound by all of the amide groups. Despite numerous attempts, involving different solvent mixtures and counter anions, the isolated crystals were all

twinned and not suitable for X-ray analysis. We have therefore investigated the solution structure of the complexes in CD_3OD by ^{13}C (Table 3) and ^{1}H (Table 4) NMR spectroscopy.

[Lu(L^1)][trif]$_3$. The ^{13}C NMR spectrum of this compound displays nine resonances in the range 212 to 333 K, characteristic of a complex with time-averaged C_4 symmetry (Fig. 2). The co-ordination environment appears to be quite rigid, including the macrocyclic ring, since two sharp signals are observed for the ring carbon atoms while the amide carbon atoms appear as one signal. The ^{1}H NMR spectrum is also temperature independent and shows nine resonances (Fig. 3) as reported for other lanthanide complexes with amide[7] or phosphinate[11] substituted tetraazacyclododecanes. A dynamic process involving the macrocyclic carbon atoms takes place at higher temperature, the corresponding signals becoming broader and closer at 333 K, a too high temperature, however, given the solvent used, to study the corresponding exchange mechanism. Proton assignments have been achieved with the help of a COSY spectrum (Fig. F1, SUP 57491) and by considering the Newman representation shown in Fig. 3. They are consistent with the above discussion. The resonances of the aromatic protons appear as a broad signal between δ 7.31 and 7.22 and the methylenic protons CH_2Ph give rise to two doublets shifted

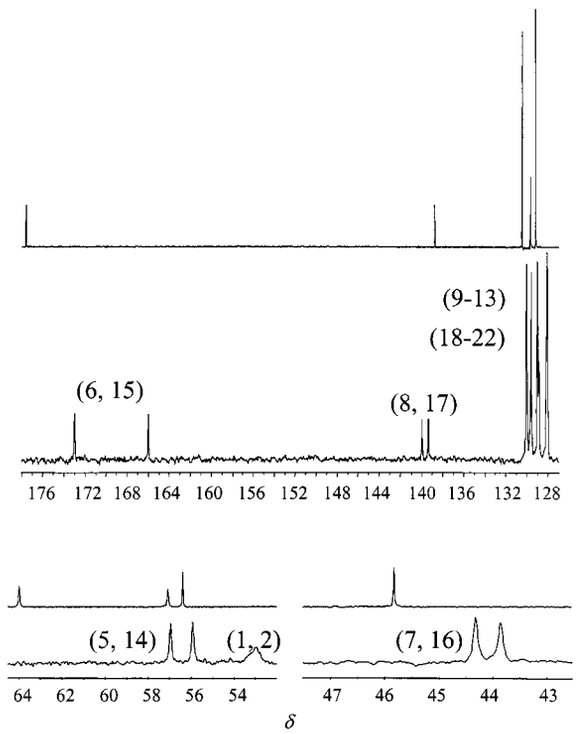

Fig. 2 ^{13}C-{^{1}H} NMR Spectra of L^1 (212 K, bottom trace) and [Lu(L^1)][trif]$_3$ (295 K, ≈10^{-2} M, top trace) in CD_3OD. The assignment refers to the numbering illustrated.

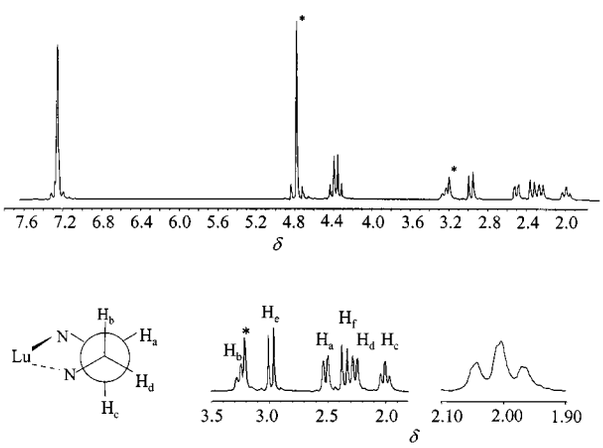

Fig. 3 The ^{1}H NMR (360.16 MHz) spectrum of [Lu(L^1)][trif]$_3$ ≈10^{-2} M in CD_3OD at 295 K. Asterisks point to the signals of the solvent (δ 3.21) and water (δ 4.80).

Table 2 Hydrogen bonding geometry in the crystal structure of L^1

Donor–hydrogen · · · acceptor	D–H/Å	H · · · A/Å	D · · · A/Å	D–H · · · A/°
N(3)–H(3A) · · · O(1)[a]	1.032	1.844	2.869(4)	171.7
N4–H(4A) · · · N(1)	1.034	2.032	2.973(4)	150.1
N4–(H4A) · · · N(2)		2.281	2.739(4)	105.1

[a] Symmetry code: $-x + 1, -y, -z + 1$.

Table 3 ^{13}C-{^{1}H} NMR Chemical shifts (δ, I_{rel}) of [LnL^1][CF_3SO_3]$_3$ (Ln = Lu or Eu) ≈ 10^{-2} M in CD_3OD (90.6 MHz, 295 K)[a]

Ln	CO	C_6H_5	NCH_2CO	ring CH_2	PhCH_2
Lu	177.6	138.8 (q, 1), 130.5 (2), 129.7 (1), 129.2 (2)	64.0 (1)	57.1 (1), 56.4 (1)	45.8 (1)
Eu	190.5	137.5 (q, 1), 129.1 (2), 128.4 (1), 127.4 (2)	75.7 (br, 1)	107.2 (1), 90.8 (1)	39.9 (1)

[a] Key: q = quaternary, br = broad; all other peaks are singlets.

Table 4 ^{1}H NMR Chemical shifts (δ, I_{rel}, J/Hz) of [LnL^1][CF_3SO_3]$_3$ (Ln = Lu or Eu) 10^{-2} M in CD_3OD (360.16 MHz, 295 K)[a]

				ring CH_2	
Ln	C_6H_5	$C_6H_5CH_2$	NCH_2CO	equatorial	axial
Lu	7.31–7.22 (5)	4.42 (d, 1), 4.35 (d, 1) ^2J = 14.8	2.98 (d, 1), 2.35 (d, 1) ^2J = 16.8	2.51 (dd, 1), 2.26 (dd, 1) $^2J_{gem(ax\text{-}eq)} = {}^3J_{ax\text{-}ax}$ = 14.5, $^3J_{ax\text{-}eq}$ = 2.1	3.24 (td, 1), 2.01 (td, 1)
Eu	6.35 (2), 6.24 (1), 6.17 (2)	2.59 (d, 1), 2.14 (d, 1) ^2J = 11.9	−13.76 (br, 1), −14.29 (br, 1)	−2.37 (1), −6.63 (1)	25.61 (1), −7.94 (1)[b]

[a] Key: d = doublet, dd = doublet of doublets, td = triplet of doublets, br = broad; other peaks are singlets; CONH protons exchange with the solvent. [b] Broad bands; assignment eq/ax impossible (see text).

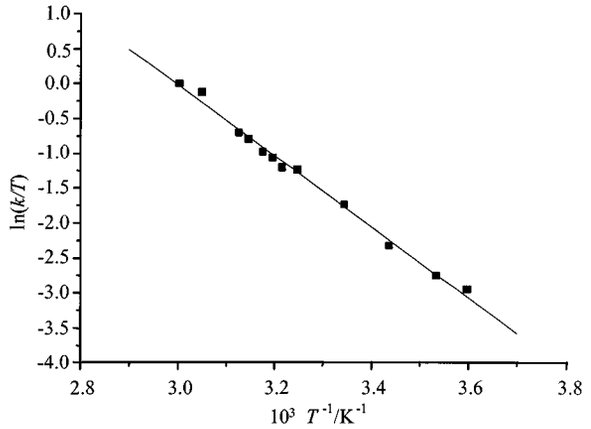

Fig. 4 Eyring plot for the benzyl rotation in $[Eu(L^1)][trif]_3$ (2.3×10^{-2} M in CD_3OD).

to lower field due to the proximity of the phenyl groups. The axial protons of the ring CH_2 groups (H_b and H_c) reveal vicinal coupling in addition to geminal coupling and appear as two triplets of doublets, while the equatorial protons (H_a, H_d) show up as two broad doublets.

$[Eu(L^1)][trif]_3$. At room temperature the ^{13}C NMR spectrum displays nine resonances, as for the lutetium(III) complex, which were assigned on the basis of a simultaneous analysis of the ^1H NMR and ^{13}C–^1H HSQC (Heteronuclear Single Quantum Coherence) spectra (Fig. F2, SUP 57491) and which again point to a time-averaged C_4 symmetry. By increasing the temperature the same phenomenon observed for the lutetium complex and involving the macrocyclic carbon atoms takes place. However, eleven resonances appear in the ^1H NMR spectrum since the aromatic protons display three signals in the range δ 6.00–6.55. The methylenic protons CH_2Ph generate two doublets, two broad signals of same intensity are observed for the NCH_2CO protons and the macrocyclic protons give rise to four broad resonances. The too short values of the transverse relaxation times of the latter (Table S2, SUP 57491) did not allow us to detect all the cross-peaks in the 2-D homonuclear COSY experiment at the frequency used (360.16 MHz) as we have done above with the lutetium complex, but comparison with similar complexes[11,12] and 1-D NOE difference experiments allowed us to assign the ring CH_2 and the NCH_2CO protons. A line shape broadening occurs upon lowering the temperature to 213 K, in line with the presence of a paramagnetic europium(III) species, but no new sets of signals are detected. This is consistent with the presence of only one isomer (>95%) in solution. The line shape of the signals does not change either upon increasing the temperature, except for the two doublets corresponding to the resonances of the CH_2Ph which undergo an exchange process with coalescence occurring at 333 K (Fig. F3, SUP 57491). This dynamic process is due to the rotation of the benzyl group around the amide N–C bond and the activation parameters determined using Eyring eqn. (1) (Fig. 4) are

$$k = (k_B T/h) \exp[-(\Delta H^{\ddagger}/RT) + (\Delta S^{\ddagger}/R)] \qquad (1)$$

$\Delta G^{\ddagger} = 57.5 \pm 0.5$ kJ mol^{-1}, $\Delta H^{\ddagger} = 43.0 \pm 0.1$ kJ mol^{-1}, $\Delta S^{\ddagger} = -49.3 \pm 0.4$ J K^{-1} mol^{-1}, with $k^{298} = 47.7 \pm 1.1$ s^{-1}. To our knowledge, no similar kinetic process has been described for this class of macrocyclic complexes. The benzyl rotation points to a tendency of the complexes to lose their structural rigidity as the ionic radius increases: the europium(III) ion seems to be less tightly encapsulated by the pendant arms than Lu^{III} and the loss of rigidity of the co-ordinating environment is certainly the cause of the very broad ^1H NMR signals observed for the ring and $N_{ring}CH_2CO$ methylenic protons of the lanthanum(III) complex, even at low temperature, which prevented us performing a detailed analysis of its NMR spectrum.

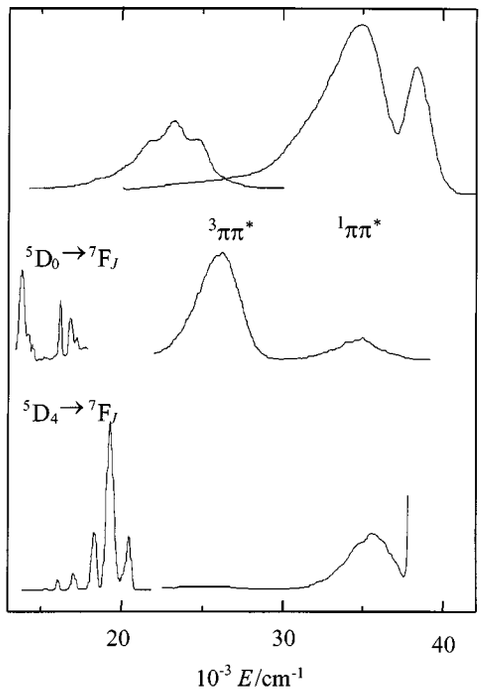

Fig. 5 Top: fluorescence (λ_{exc} = 259 nm, bandpath = 8 nm, 295 K) and phosphorescence (λ_{exc} = 270 nm, bandpath = 10 nm, delay time = 50 μs, 77 K) spectra of solid L^1. Middle: phosphorescence of $[Eu(L^1)][trif]_3$ (λ_{exc} = 240 nm, bandpath = 6 nm, delay time = 20 μs). Bottom: phosphorescence of $[Tb(L^1)][trif]_3$ (left, λ_{exc} = 258 nm, bandpath = 6 nm, delay time = 20 μs); ligand-centred emission of $[Tb(L^1)][trif]_3$ (lower trace right, λ_{exc} = 258 nm, bandpath = 2.5 nm); solid state, 77 K. Vertical scale: arbitrary units.

Relaxivity measurements on $[Gd(L^1)][trif]_3$

We have measured relaxivity *versus* pH and it parallels the behaviour described for the gadolinium complex with DTMA [tetrakis(methylamide) of 1,4,7,10-tetraazacyclododecane-1,4,7,10-tetraacetate].[13a,b] At 10 MHz and 298 K the gadolinium complex displays the following relaxivities at pH 0.8, 1.0, 6.7 and 11.1: 4.08, 2.08, 1.88 and 6.14 mM^{-1} s^{-1}, respectively. The enhancement of the relaxivity at basic pH can be explained by a prototropic exchange catalysed by OH^-. For acidic pH the measurements were started 3 h after preparing the solutions. Taking this into account, the increase in relaxivity can be explained by the protonation of the complex which results in a weakening of the N–Gd bond as recently reported for $[Gd(DTMA)]^{3+}$,[13b] and allows an easy diffusion of water molecules around the gadolinium(III) ion.

Photophysical properties

The absorption spectrum of L^1 in MeCN displays the characteristic $\pi \longrightarrow \pi^*$ transitions of the C=O groups at 52 630 cm^{-1} ($\varepsilon \approx 190\,000$ M^{-1} cm^{-1}; shoulder at 47 620 cm^{-1}, $\varepsilon \approx 45\,000$ M^{-1} cm^{-1}) and phenyl groups at 38 760 cm^{-1} ($\varepsilon \approx 800$ M^{-1} cm^{-1}). Absorption and reflectance spectra of the complexes show the same bands, with small shifts only (Fig. F4, SUP 57491). The luminescence spectrum of L^1 in the solid state (77 K, Fig. 5) is comprised of two transitions, assigned to the lowest $^1\pi\pi^*$ and $^3\pi\pi^*$ states: the former lies at 31 250 cm^{-1} while the latter occurs at 23 250 cm^{-1} (maxima of the band envelopes). The emission band corresponding to the $^3\pi\pi^*$ state displays a vibrational progression of about 1400 cm^{-1}, probably corresponding to a ring breathing mode, and the 0-phonon transition could be located at 26 300 cm^{-1}. In frozen solution in acetonitrile (77 K, 10^{-4} M), the emission maximum of the singlet state is found at

Table 5 Observed radiative rate constants of the Eu($^5D_0$) and Tb($^5D_4$) excited levels in [Ln(L^1)][trif]$_3$ under various experimental conditions

Ln	Conditions	T/K	Excitation	k/ms^{-1}
Eu	Solid	10	$^5D_0 \longleftarrow {}^7F_0$	0.81 ± 0.02
	Solid	295	$^5D_0 \longleftarrow {}^7F_0$	0.85 ± 0.02
	9×10^{-4} M/MeCN	295	Ligand $^1\pi\pi^*$	0.78 ± 0.01
	9×10^{-4} M/MeCN–water[a]	295	Ligand $^1\pi\pi^*$	1.69 ± 0.03
	6.6×10^{-4} M/water	295	Ligand $^1\pi\pi^*$	1.54 ± 0.01
	5.9×10^{-4} M/D_2O	295	Ligand $^1\pi\pi^*$	0.41 ± 0.02
Tb	Solid	77	Ligand $^1\pi\pi^*$	0.53 ± 0.01
	Solid	295	Ligand $^1\pi\pi^*$	0.53 ± 0.02
	1.1×10^{-3} M/MeCN	295	Ligand $^1\pi\pi^*$	0.51 ± 0.04
	1.1×10^{-3} M/MeCN–water[a]	295	Ligand $^1\pi\pi^*$	0.68 ± 0.06
	6.1×10^{-4} M/water	295	Ligand $^1\pi\pi^*$	0.66 ± 0.04
	6.8×10^{-4} M/D_2O	295	Ligand $^1\pi\pi^*$	0.35 ± 0.02

[a] $[H_2O]_t/[Ln^{III}]_t = 2000$.

34 840 cm^{-1} and the band corresponding to the emission of the $^3\pi\pi^*$ state is structureless with a maximum at 23 250 cm^{-1}. No emission arising from an excimer could be detected in the fluorescence spectra, contrary to what was found for a similar ligand bearing naphthalene moieties,[14] meaning that the interaction between the phenyl groups observed in the crystal structure is not very strong. The lifetime of the triplet state amounts to 0.62 ± 0.01 s in the solid state and 1.03 ± 0.01 s in MeCN at 77 K. In frozen solutions of the complexes of La^{III} and Lu^{III}, 10^{-4} M in MeCN, the maximum of the triplet state is blue shifted at 23 100 (La) and 22 700 cm^{-1} (Lu) and the lifetime becomes shorter: 0.93 ± 0.01 (La) and 0.86 ± 0.02 s (Lu).

When luminescent ions such as Eu^{III} and Tb^{III} are introduced into the macrocyclic edifices the luminescence spectra display a mixture of ligand-centred band emission and metal-centred line emission (Fig. 5). For [Tb(L^1)][trif]$_3$ the ligand-to-metal energy transfer is fairly efficient and the low-temperature spectrum is dominated by strong $^5D_4 \longrightarrow {}^7F_J$ transitions while a sizable emission from the $^1\pi\pi^*$ state is still observed, but the $^3\pi\pi^*$ state emits very weakly. The lifetime of the Tb($^5D_4$) excited state is relatively long and temperature independent (Table 5), pointing to an absence of back transfer, a process commonly observed for Tb^{III} containing edifices.[15] Furthermore, the quantum yield of a 10^{-3} M solution in degassed MeCN has been measured relatively to [Tb(terpy)][ClO_4]$_3$ (terpy = 2,2′:6′,2″-terpyridine; absolute quantum yield 4.8%[15]) and found to be 1.36 (absolute quantum yield: 6.4%). Although the intersystem crossing between $^1\pi\pi^*$ and $^3\pi\pi^*$ states is not complete [*cf.* the ligand-centred emission band in the spectrum of the terbium(III) complex], L^1 is a fairly efficient ligand to sensitize the Tb^{III}-centred luminescence. This was expected from the correlation between the lowest triplet state energy of the ligand and the terbium(III) quantum yield recently published by Latva *et al.*[16] for several polyaminocarboxylate chelates, in which the authors show triplet states with energy between *ca.* 22 000 and 27 000 cm^{-1} being the most efficient sensitizers of Tb^{III}. Benzyl substituted cyclenes have also been described as good sensitizers of Tb^{III} when the systems lack the presence of closely diffusing OH and CO oscillators.[11,17]

On the other hand, energy transfer from the $^3\pi\pi^*$ state to the europium(III) excited states is quite poor and the luminescence spectrum of [Eu(L^1)][trif]$_3$ displays weak $^5D_0 \longrightarrow {}^7F_J$ transitions besides sizable $^3\pi\pi^*$ and $^1\pi\pi^*$ state emission. This is somewhat surprising because for polyaminocarboxylate chelates a triplet state with an energy of about 27 000 cm^{-1} was shown to transfer reasonably well its energy onto the ^5L_J manifold.[16] The effectiveness of the ligand for energy transfer to Ln^{III} and the quantum yield of the metal-centred luminescence also depend on many other factors. In particular, the europium(III) ion is easily reduced to Eu^{II}, with the intermediate formation of a radical cation, by photoinduced electron transfer (PET) from the singlet state of the ligand directly to the metal, as has been observed for other tetraazamacrocyclic compounds with pendant arms bearing amide[18] or phosphinate[17] functions and for triple helical complexes with bis(benzimidazole)pyridines.[19] The quantum yield of the europium(III) complex relative to [Eu(terpy)][ClO_4]$_3$ is very small (≈5×10^{-2}), which corresponds to an absolute quantum yield of about 0.06%. These observations are opposite to those reported for complexes with an octadentate tetraazamacrocyclic ligand bearing naphthyl chromophores, where the differences between the triplet and the excited metal ion states are respectively 750 (Tb^{III}) and 3900 cm^{-1} (Eu^{III}): transfer onto the europium(III) ion is efficient while a back transfer process takes place for Tb^{III}.[14]

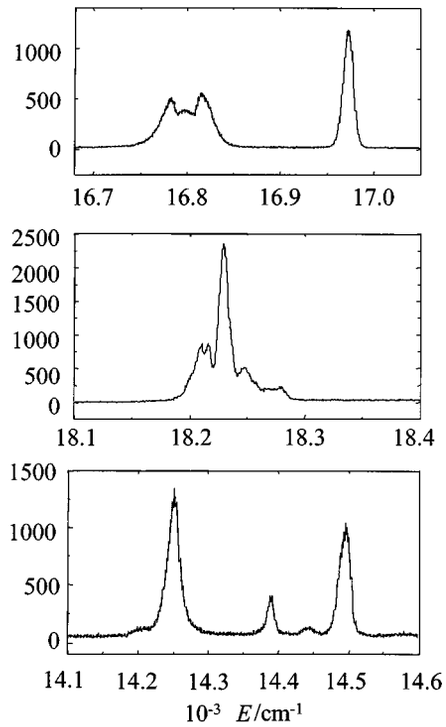

Fig. 6 Corrected emission spectra of the $^5D_0 \longrightarrow {}^7F_1$ (top), $^5D_0 \longrightarrow {}^7F_2$ (middle) and $^5D_0 \longrightarrow {}^7F_4$ (bottom) transitions of [Eu(L^1)][trif]$_3$ at 10 K under selective laser excitation (17 234 cm^{-1}, bandpath = 0.3 Å).

Structural properties of [Eu(L^1)][trif]$_3$ as probed by luminescence measurements. High resolution excitation and emission spectra have been recorded at 10, 77 and 295 K to probe the site symmetry of the europium(III) environment. Broad band excitation at 397 nm ($^5L_6 \longleftarrow {}^7F_{0,1}$ transitions) yields an emission spectrum in which the corrected relative intensities for the $^5D_0 \longrightarrow {}^7F_J$ transitions to $J = 0$, 1, 2, 3 and 4 are 0.19, 1.00, 1.36, 0.04 and 1.64, respectively. Selective excitation at 580.24 nm ($^5D_0 \longleftarrow {}^7F_0$ transition) yields the spectrum in Fig. 6, which is almost temperature independent, so that only the 10 K data are discussed below. The laser excited excitation spectrum of the 0–0 transition recorded upon monitoring the high energy component of the $^5D_0 \longrightarrow {}^7F_1$ transition displays one symmetrical band at 17 234 cm^{-1} with a full width at half height (fwhh) of 12 cm^{-1} (Fig. F5, SUP 57491). When the europium(III) ion lies in a rigid and well defined site the fwhh of this transition is usually only a few cm^{-1}.[20] The moderately large fwhh observed here probably arises from slightly different metal environments, as often observed for microcrystalline materials.[21] In fact, when the observation wavelength is set onto the various emission bands of the spectrum displayed in Fig. 6, the 0–0 transition spans an energy range between 17 225 and 17 245 cm^{-1}, consistent with the above interpretation. Moreover, laser excitation between these wavenumbers yielded essentially similar spectra, the transitions displaying a shift varying linearly with the excitation energy.

Table 6 Identified electronic and vibronic transitions in the luminescence spectrum of $[Eu(L^1)][trif]_3$ (solid state, 10 K, excitation: $^5D_0 \longleftarrow\!\!\!- {}^7F_0$ transition)

E/cm^{-1}	Intensity[a]	E^*/cm^{-1}	Transition[b]
17 234	m	0	$^5D_0 \longrightarrow {}^7F_0$
16 971	m	263	$^5D_0 \longrightarrow {}^7F_1$
16 814	w	420	$^5D_0 \longrightarrow {}^7F_1$
16 797	w	437	Vibronic (420)[b]
16 779	w	455	$^5D_0 \longrightarrow {}^7F_1$
16 267	sh	967	Vibronic (970)[b]
16 257	m	977	$^5D_0 \longrightarrow {}^7F_2$
16 252	m	982	$^5D_0 \longrightarrow {}^7F_2$
16 238	vs	996	$^5D_0 \longrightarrow {}^7F_2$
16 221	w	1013	Vibronic (1022)[b]
16 211	sh	1023	Vibronic (1031)[b]
16 189	vw	1045	Vibronic (1038)[b]
15 274	vw	1960	$^5D_0 \longrightarrow {}^7F_3$
14 490	m	2744	$^5D_0 \longrightarrow {}^7F_4$
14 437	vw	2797	$^5D_0 \longrightarrow {}^7F_4$
14 381	w	2853	$^5D_0 \longrightarrow {}^7F_4$
14 243	m	2991	$^5D_0 \longrightarrow {}^7F_4$

[a] s = Strong, m = medium, w = weak, vw = very weak, sh = shoulder. [b] The IR data are given in parentheses.

The symmetry of the europium(III) ion has been determined as follows. First, the intensity of the $^5D_0 \longrightarrow {}^7F_0$ transition is particularly large, pointing to a C_n (or C_{nv}) point group of symmetry. Given the formulation of the complex, the only feasible point groups are C_4 and C_{4v}. Group theoretical considerations predict the same number of transitions from the $^5D_0$ excited state to the ^7F_J manifold for $J = 0$, 1 and 2 (subscripts refer to C_{4v}):[20] 1 ($A_{(1)}$), 2 ($A_{(2)}$ + E), 2 ($A_{(1)}$ + E), so that a distinction can only be made by analysing the transition to $J = 4$ for which C_4 allows 5 transitions (3A + 2E) and C_{4v} 4 transitions ($2A_1$ + 2E). Selectively excited spectra ($^5D_0 \longleftarrow\!\!\!- {}^7F_0$) have been recorded to determine the number of components for each $^5D_0 \longrightarrow {}^7F_J$ transition ($J = 1$, 2 and 4, Fig. 6). The $^5D_0 \longrightarrow {}^7F_1$ transition displays 3 components, two of them appearing as a doublet with a splitting of 35 cm^{-1}; additionally, the transition contains a vibronic component at 437 cm^{-1} (Table 6). Analysis of the hypersensitive transition to $J = 2$ is more difficult since it is essentially comprised of one intense and sharp transition and of six weak components, several of which can be assigned to vibronic transitions (Table 6); we assign tentatively the more intense band to an A-type transition and the doublet (spacing 5 cm^{-1}) on its high energy side to an E-type transition. Finally, the $^5D_0 \longrightarrow {}^7F_4$ transition displays three sizable components and two very weak ones. Globally, therefore, the emission spectra are consistent with a slightly distorted C_4 symmetry, which splits the E components of the transitions to $J = 1$, 2 into two components. The distortion may occur in the ground or in the excited state, but we note that a distorted square antiprismatic co-ordination geometry has been found by X-ray analysis for the lanthanum(III) complex with 1,4,7,10-tetrakis(2-carbamoylethyl)-1,4,7,10-tetraazacyclododecane.[22] Finally, no changes are observed in the emission spectra of the europium(III) ion for $[Ln_{0.98}Eu_{0.02}(L^1)][trif]_3$ (Ln = La, Eu, Gd or Lu) compounds in the solid state, pointing to an isotypical series of edifices, with pseudo-C_4 symmetry.

Frey and Horrocks[23] recently proposed a correlation between the energy of the 0–0 transition, that is the position of the $^5D_0$ level, and parameters describing the ability δ of co-ordinating atoms to produce a nephelauxetic effect: $\tilde{\nu} - \tilde{\nu}_0 = C_{CN}\Sigma_i n_i\delta_i$ where C_{CN} is a coefficient depending upon the europium(III) co-ordination number (1.06 for CN = 8, 1.0 for CN = 9), n_i the number of atoms of type i, and $\tilde{\nu}_0 = 17\,374$ cm^{-1} at 295 K; the parameters δ are tabulated for several functional groups. We have recently demonstrated that a heterocyclic N atom (HN) tends to produce a larger nephelauxetic effect than a primary amine (−12.1) and have deduced from our work on nine-co-ordinate triple-helical complexes with the benzimidazole-containing ligands a δ_{HN} parameter equal to −15.3.[24] Taking the latter value into account, as well as $\delta_{amide} = -15.7$ and $C_{CN} = 1.06$,[23] we find 17 243 cm^{-1} for $[Eu(L^1)]^{3+}$, while the experimental value at 295 K is 17 246 cm^{-1}. This result is therefore consistent with no bound water molecule in the first co-ordination sphere, which can be explained by the vigorous drying performed after isolation of the complexes (60 °C, 1 mbar, 12 h). That no water is co-ordinated to Eu^{III} is corroborated by the small radiative rate constant observed for the $^5D_0$ excited state between 10 and 295 K in the solid state (0.81 and 0.85 ms^{-1} respectively, Table 5). A similar value holds for a solution 10^{-3} M in dry MeCN; however, when water is added ($[H_2O]_t/[Eu^{III}]_t = 2000$) the rate constant increases in a proportion corresponding to a number of bound water molecules $q = 0.96$, as calculated by Horrocks' equation,[25] which increases to $q = 1.19$ in water. Under these experimental conditions, the ninth co-ordination position is occupied by a water molecule. For the terbium(III) complex q increases from 0.71 in aqueous MeCN to 1.30 in pure water. Taking into account the corrections proposed by Dickins *et al.*[5] for closely diffusing OH [$\Delta k'(Eu) = -0.25$, $\Delta k'(Tb) = -0.06$ ms^{-1}] and NH [$\Delta k'(Eu) = -0.08$ ms^{-1}], and their new formulation of Horrock's equation, $q' = A'(\Delta k + \Delta k')$ with $A'(Eu) = 1.25$ and $A'(Tb) = 4.9$, we find the following data: $q'(Eu) = 0.43$ (aqueous MeCN) and 0.70 (H_2O), $q'(Tb) = 0.54$ (aqueous MeCN) and 1.23 (H_2O).

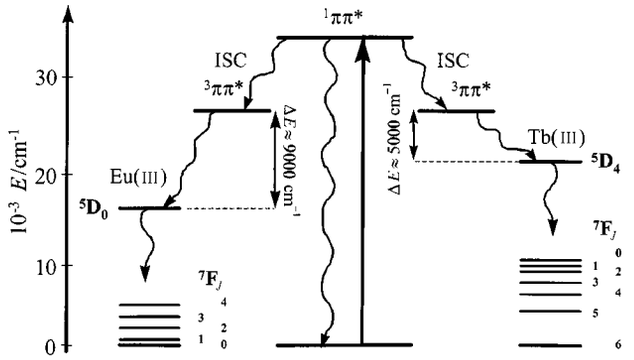

Fig. 7 Energy migration scheme for $[Ln(L^1)][trif]_3$ complexes (Ln = Eu or Tb).

Conclusion

We have shown that ligand L^1 adopts a twofold symmetry both in the solid state and in solution, in which rapid movements of the macrocyclic ring and the pendant arms occur. The ligand provides a tight co-ordination cage for the heavier lanthanide(III) ions, as demonstrated by a detailed NMR analysis of the diamagnetic lutetium(III) complex. For both complexes of Lu^{III} and Eu^{III} only one C_4-symmetric isomer is present in solution and no exchange process is evidenced in the temperature range studied (212–323 K), as observed for similar europium(III) compounds. In addition, the rotation of the benzyl groups in $[Eu(L^1)][trif]_3$, quantified by a dynamic NMR analysis, and the broad NMR signals generated by the lanthanum(III) complex lead to the conclusion that the structure becomes somewhat fluxional for larger lanthanum(III) ions. Luminescence data demonstrate that L^1 is a suitable ligand for sensitizing Tb^{III}, but not Eu^{III}, because the energy of its lowest triplet state (26 300 cm^{-1} for the 0-phonon transition in the solid state) is about 5000 cm^{-1} higher than the $^5D_4$ level and so no back transfer is observed in $[Tb(L^1)][trif]_3$ (Fig. 7). On another hand, the internal conversion from the singlet to the triplet state appears to be insufficient to ensure large quantum yields. However, a comparison with literature data on similar compounds

shows that the physical properties of the lanthanide edifices with [12]aneN$_4$ ligands may be easily tuned by changing the nature of the pendant arm properties, which offers interesting perspectives for the development of efficient luminescent stains.

Experimental

Starting materials, procedures and spectroscopic measurements

Solvents and chemicals were purchased from Fluka AG (Buchs, Switzerland). Acetonitrile was treated by CaH_2 and P_2O_5.[26] Dichloromethane and tetrahydrofuran were distilled from CaH_2. Lanthanide trifluoromethanesulfonates (triflates) were prepared from the oxides (Rhône-Poulenc, 99.99%) and triflic acid.[27] Elemental analyses were performed by Dr H. Eder of the Microchemical Laboratory of the University of Geneva. Electrospray mass spectra (ES-MS) were measured on a Finnigan SSQ-710C spectrometer driven by a Digital Personal DEC station 5000/25. Geometry calculations have been performed by PLATON 98.[28]

The 1- and 2-D NMR spectra were recorded on a Bruker AM-360 (360.16 and 90.6 MHz respectively) or on a Bruker Avance DRX-400 spectrometer (400.03 and 100.04 MHz). Proton chemical shifts are reported in parts per million (ppm) with respect to TMS, and ^{13}C chemical shifts are related to CD_3OD (δ 49.3). We have chosen CD_3OD as NMR solvent because in CD_3CN signals became broader, pointing to an interaction between the complexes and the solvent as described previously.[29] Activation parameters have been obtained by fitting spectra using the program NMRICMA.[30] All the ligand solution studies have been achieved with added protons ($CF_3SO_3H \approx 1$–5 μM). Relaxivity measurements have been performed at 10 MHz with a Stelar fast field cycling Spinmaster relaxometer equipped with a Stelar VTC-91 air flow heating unit. For both NMR and relaxivities measurements the temperature was measured by a substitution technique.[31] Electronic UV-VIS-NIR spectra were recorded at 295 K on a Perkin-Elmer Lambda 900 spectrometer, infrared spectra on a FT-IR Mattson Alpha Centauri spectrometer (4000–400 cm^{-1}, KBr pellets) and on a Bruker IFS-113v FT-IR interferometer (700–100 cm^{-1}, polyethylene pellets). Low-resolution luminescence measurements (spectra and lifetimes) were recorded on a Perkin-Elmer LS-50B spectrofluorimeter. High-resolution spectra and lifetimes of the europium complexes in the solid state were measured on a previously described instrumental set-up;[32] lifetimes were averages of at least four determinations. Quantum yields of [Tb(L^1)][trif]$_3$ and [Eu(L^1)][trif]$_3$ were determined in anhydrous and degassed MeCN relative to [Tb(terpy)$_3$][ClO$_4$]$_3$ and [Eu(terpy)$_3$][ClO$_4$]$_3$ respectively,[33] with the help of a Perkin-Elmer LS-50B spectrofluorimeter.

Syntheses and characterization

1,4,7,10-Tetraazacyclododecane was synthesized as previously described.[29] *N*-Benzylbromoacetamide was prepared using the method of Hamada *et al.*[34] with bromoacetyl chloride instead of chloroacetyl chloride. The yield is 70%. TLC: 1 spot, $R_f = 0.8$ (5% MeOH in $CHCl_3$). δ_H ($CDCl_3$) 3.92 (s, 2 H, $BrCH_2$), 4.43 and 4.50 (dd, $^2J = 16.6$ Hz, 2 H, NCH_2Ph), 6.74 (s, br, 1 H, NH) and 7.30 (m, 5 H, aryl). mp 110 °C.

1,4,7,10-Tetrakis(*N*-benzylcarbamoylmethyl)-1,4,7,10-tetraazacyclododecane (L^1). A mixture of 1 equivalent of 1,4,7,10-tetraazacyclododecane (113.2 mg, 0.66 mmol), 4 equivalents of *N*-benzylbromoacetamide (599.5 mg, 2.64 mmol) and 4 equivalents of triethylamine (0.37 ml, 2.64 mmol) in dry THF was refluxed under nitrogen during 7 h. The deposited solid was recovered by filtration and washed with 500 ml water portions until negative reaction of the filtrate with $AgNO_3$, and with 100 ml EtOH. It was purified by recrystallization from acetonitrile (yield 60%) (Found: C, 69.62; H, 7.21; N, 14.48. $C_{11}H_{14}N_2O$ requires C, 69.45; H, 7.42; N, 14.72%). ES-MS (10^{-4} mol dm^{-3} in MeCN + CF_3SO_3H): two peaks at $m/z = 762.0$ (L^{1}H$^+$) and 381.2 (L^{1}H$_2^{2+}$). $\delta_C\{^1H\}$ (90.6 MHz, CD_3OD + CF_3SO_3H, 212 K) 173.0 (1C, CO), 166.0 (1C, CO), 140.0 (1C, aryl), 139.4 (1C, aryl), 130.0 (2C, aryl), 129.6 (2C, aryl), 129.0 (2C, aryl), 128.9 (1C aryl), 128.1 (2C + 1C, aryl), 57.0 (1C, N*C*H$_2$CO), 55.9 (1C, N*C*H$_2$CO), 52.9 (4C, br, ring CH$_2$), 44.3 (1C, CH$_2$Ph) and 43.8 (1C, CH$_2$Ph). IR: ν_{max} 3304 (N–H), 1651 and 1662 cm^{-1} (C=O).

Complexes. The complexes [Ln(L^1)][trif]$_3$ were prepared by heating under reflux 1 equivalent of the lanthanide salt and 1 equivalent of L^1 in dry MeCN. After cooling, the solution was filtered on sintered glass and concentrated, CH_2Cl_2 was added and the resulting solution kept for 10 h at 277 K. The deposited solid was recovered by filtration, washed with CH_2Cl_2 and dried (2 h, 1 mbar, 313 K). The complexes were recrystallized from MeCN (yield ≈ 70%).

[La(L^1)][trif]$_3$ (Found: C, 41.78; H, 4.13; N, 8.19. Calc. for $C_{47}H_{56}F_9LaN_8O_{13}S_3$: C, 41.91; H, 4.19; N, 8.35%). $\delta_C\{^1H\}$ (CD_3OD, 295 K) 177.1 (1C, CO), 138.6 (1C, aryl), 130.3 (2C, aryl), 129.5 (1C, aryl), 129.4 (2C, aryl), 61.9 (1C, N*C*H$_2$CO), 56.0 (br, 1C, ring CH$_2$), 53.2 (br, 1C, ring CH$_2$) and 45.8 (1C, CH$_2$Ph). IR: ν_{max} 3264 (N–H) and 1627 cm^{-1} (C=O).

[Nd(L^1)][trif]$_3$ (Found: C, 41.69; H, 4.23; N, 8.20. Calc. for $C_{47}H_{56}F_9N_8NdO_{13}S_3$: C, 41.74; H, 4.17; N, 8.29%). IR: ν_{max} 3265 (N–H) and 1629 cm^{-1} (C=O).

[Eu(L^1)][trif]$_3$ (Found: C, 41.49; H, 4.09; N, 8.20. Calc. for $C_{47}H_{56}EuF_9N_8O_{13}S_3$: C, 41.50; H, 4.15; N, 8.24%). ν_{max} 3268 (N–H) and 1632 cm^{-1} (C=O).

[Gd(L^1)][trif]$_3$ (Found: C, 41.27; H, 4.20; N, 8.17. Calc. for $C_{47}H_{56}F_9GdN_8O_{13}S_3$: C, 41.34; H, 4.13; N, 8.21%).

[Tb(L^1)][trif]$_3$ (Found: C, 41.12; H, 4.11; N, 8.15. Calc. for $C_{47}H_{56}F_9N_8O_{13}S_3Tb$: C, 41.28; H, 4.13; N, 8.20%). IR: ν_{max} 3270 (N–H) and 1634 cm^{-1} (C=O).

[Lu(L^1)][trif]$_3$ (Found: C, 40.57; H, 4.04; N, 8.05. Calc. for $C_{47}H_{56}F_9LuN_8O_{13}S_3$: C, 40.82; H, 4.08; N, 8.10%). ν_{max} 3273 (N–H) and 1639 cm^{-1} (C=O).

Crystal structure of L^1

A transparent single crystal of L^1 was mounted on a pin and transferred to the goniometer. The crystal was cooled to −100 °C during data collection by using a stream of cold nitrogen gas. The monoclinic space group $P2_1/c$ was uniquely determined by the systematic absences. A summary of data collection and refinement parameters is given in Table 7. The geometrically constrained hydrogen atoms were placed in calculated positions and allowed to ride on their attached atoms with $B = 1.2U_{eq}$(C). The two unique NH hydrogen atoms were located from a Fourier difference map and allowed to ride on the bonded atom with $B = 1.2U_{eq}$(N). Refinement of non-hydrogen atoms was carried out with anisotropic thermal parameters. Drawings were made using the ORTEP 3 program package.[37]

CCDC reference number 186/1326.

See http://www.rsc.org/suppdata/dt/1999/931/ for crystallographic files in .cif format.

Acknowledgements

This research is supported by grants from the Swiss National Science Foundation and the Swiss Federal Office for Science and Education (COST project D8). We thank the Fondation Herbette (Lausanne) for spectroscopic equipment, F. Monlien for her assistance in using the NMRICMA program, F. Dunan for relaxivity measurements, D. Baumann for recording far-IR spectra and V. Foiret for her help in the acquisition of some luminescence data.

Table 7 Summary of crystal data, data collection, structure solution and refinements details for L^1 [a]

Formula	$C_{44}H_{56}N_8O_4$
M	760.97
Colour, habit	Colourless, plate
Crystal size/mm	0.06 × 0.18 × 0.22
Crystal system	Monoclinic
Space group	$P2_1/c$
a/Å	13.0360(11)
b/Å	16.1964(14)
c/Å	9.7490(9)
β/°	97.117(3)
U/Å^3	2042.5(3)
Z	2
F(000)	816
D_c/g cm^{-3}	1.237
μ/mm^{-1}	0.081
Unit-cell reflections (θ range/°)	1610 (1.57 to 24.68)
hkl Ranges	−13 to 15, −18 to 19, −7 to 11
Reflections measured	10 230
Unique reflections	3461 (R_{int} = 0.1091)
Reflections with $I > 2\sigma$	1716
Absorption correction	SADABS [35]
Extinction coefficient	0.013(2)
Refinement method	Full-matrix least squares on F^2, no restraints
Solution method	Direct methods
No. variables	254
Goodness of fit on F^2	1.027
Final $R1$, $wR2$ indices ($I \geq 2\sigma$)	0.0733, 0.1174
(all data)	0.1815, 0.1732
Density range in final map/e Å^{-3}	0.213 and −0.208

[a] Data collection on a Siemens SMART instrument with CCD area detector and graphite monochromatized Mo-Kα radiation (λ = 0.71073 Å). Computing was done with SHELXTL.[36]

References

1 R. B. Lauffer, *MRI Clinical Magnetic Resonance Imaging*, eds. R. E. Edelman, M. B. Zlatkin and J. R. Hesselink, W. B. Saunders Co, Philadelphia, 1996, vol. 1, ch. 5.
2 S. Aime, M. Botta, R. S. Dickins, C. L. Maupin, D. Parker, J. P. Riehl and J. G. Williams, *J. Chem. Soc.*, *Dalton Trans.*, 1998, 881.
3 G. L. DeNardo, G. R. Mirick, L. A. Kroger, R. T. O'Donnell, C. F. Meares and S. J. DeNardo, *J. Nucl. Med.*, 1996, **37**, 451.
4 L. L. Chappell, D. A. Voss, W. d. J. Horrocks and J. R. Morrow, *Inorg. Chem.*, 1998, **37**, 3989.
5 R. S. Dickins, T. Gunnlaugsson, D. Parker and R. D. Peacock, *Chem. Commun.*, 1998, 1643.
6 D. Parker, K. Senanayake and J. A. G. Williams, *J. Chem. Soc.*, *Perkin Trans. 2*, 1998, 2129.
7 J. H. Forsberg, R. M. Delaney, Q. Zhao, G. Harakas and R. Chandran, *Inorg. Chem.*, 1995, **34**, 3705.
8 J.-C. G. Bünzli, *Lanthanide Probes in Life, Chemical and Earth Sciences. Theory and Practice*, eds. J.-C. G. Bünzli and G. R. Choppin, Elsevier, Amsterdam, 1989, ch. 7, p. 219.
9 (*a*) A. Beeby, D. Parker and J. A. G. Williams, *J. Chem. Soc.*, *Perkin Trans. 2*, 1996, 1565; (*b*) R. S. Dickins, J. A. K. Howard, C. L. Maupin, J. M. Moloney, D. Parker, R. D. Peacock, J. P. Riehl and G. Siligardi, *New J. Chem.*, 1998, 891.
10 R. S. Dickins, J. A. K. Howard, C. W. Lehmann, J. Moloney, D. Parker and R. D. Peacock, *Angew. Chem.*, *Int. Ed. Engl.*, 1997, **38**, 521.
11 S. Aime, A. S. Batsanov, M. Botta, J. A. K. Howard, D. Parker, K. Senanayake and J. A. G. Williams, *Inorg. Chem.*, 1994, **33**, 4696.
12 S. Aime, M. Botta, D. Parker and J. A. G. Williams, *J. Chem. Soc.*, *Dalton Trans.*, 1995, 2259.
13 (*a*) S. Aime, A. Barge, M. Botta, D. Parker and A. S. de Sousa, *J. Am. Chem. Soc.*, 1997, **119**, 4767; (*b*) L. Alderighi, A. Bianchi, L. Calabi, P. Dapporto, C. Giorgi, P. Losi, L. Paleari, P. Paoli, P. Rossi, B. Valtancoli and M. Virtuani, *Eur. J. Inorg. Chem.*, 1998, 1581.
14 D. Parker and J. A. G. Williams, *J. Chem. Soc.*, *Perkin Trans. 2*, 1995, 1305.
15 L. J. Charbonnière, C. Balsiger, K. J. Schenk and J.-C. G. Bünzli, *J. Chem. Soc.*, *Dalton Trans.*, 1998, 505.
16 M. Latva, H. Takalo, V. M. Mukkala, C. Matachescu, J.-C. Rodriguez-Ubis and J. Kankare, *J. Lumin.*, 1997, **75**, 149.
17 S. Aime, A. S. Batsanov, M. Botta, R. S. Dickins, S. Faulkner, C. E. Foster, A. Harrison, J. A. K. Howard, J. M. Moloney, T. J. Norman, D. Parker, L. Royle and J. A. G. Williams, *J. Chem. Soc.*, *Dalton Trans.*, 1997, 3623.
18 D. Parker and J. A. G. Williams, *J. Chem. Soc.*, *Dalton Trans.*, 1996, 3613.
19 S. Petoud, T. Glanzmann, J.-C. G. Bünzli, C. Piguet, Qin Xiang and R. P. Thummel, *J. Lumin.*, 1999, in the press.
20 J.-C. G. Bünzli, *Lanthanide Probes in Life, Chemical and Earth Sciences. Theory and Practice*, eds. J.-C. G. Bünzli and G. R. Choppin, Elsevier, Amsterdam, 1989, ch. 7, pp. 219–293.
21 F. Nicolo, D. Plancherel, G. Chapuis and J.-C. G. Bünzli, *Inorg. Chem.*, 1988, **27**, 3518.
22 J. R. Morrow, S. Amin, C. H. Lake and M. R. Churchill, *Inorg. Chem.*, 1993, **32**, 4566.
23 S. T. Frey and W. d. J. Horrocks, *Inorg. Chim. Acta*, 1995, **229**, 383.
24 N. Martin, J.-C. G. Bünzli, V. McKee, C. Piguet and G. Hopfgartner, *Inorg. Chem.*, 1998, **37**, 577.
25 W. DeW. Horrocks, Jr. and D. R. Sudnik, *Acc. Chem. Res.*, 1981, **14**, 384.
26 D. D. Perrin and W. L. F. Armarego, *Purification of Laboratory Chemicals*, Pergamon, Oxford, 1988.
27 J.-C. G. Bünzli and F. Pilloud, *Inorg. Chem.*, 1989, **28**, 2638.
28 L. J. Farrugia and T. Spek, PLATON 98 for Windows, 1998.
29 P. A. Pittet, D. Früh, V. Tissières and J.-C. G. Bünzli, *J. Chem. Soc.*, *Dalton Trans.*, 1997, 895.
30 L. Helm, NMRICMA, version 2.03, Library of the Institute of Inorganic and Analytical Chemistry, University of Lausanne, 1998.
31 C. Amman, P. Meier and A. E. Merbach, *J. Magn. Reson.*, 1982, **46**, 319.
32 J.-C. G. Bünzli and A. Milicic-Tang, *Inorg. Chim. Acta*, 1996, **252**, 221.
33 S. Petoud, J.-C. G. Bünzli, K. J. Schenk and C. Piguet, *Inorg. Chem.*, 1997, **36**, 1345.
34 T. Hamada, Y. Okuno, M. Ohmori, T. Niski and O. Yonemitsu, *Chem. Pharm. Bull.*, 1981, **29**, 128.
35 G. M. Sheldrick, SADABS, Program for semiempirical absorption correction of area detector data, University of Göttingen, 1996.
36 G. M. Sheldrick, SHELXTL, version 5.05, Siemens Analytical X-Ray Instruments Inc., Madison, WI, 1996.
37 L. J. Farrugia, *J. Appl. Crystallogr.*, 1997, **30**, 565.

Paper 8/09459D